

# Bioenergetic Mechanisms in Astrocytes May Contribute to Amyloid Plaque Deposition and Toxicity\*

Received for publication, October 10, 2014, and in revised form, March 20, 2015. Published, JBC Papers in Press, March 26, 2015, DOI 10.1074/jbc.M114.618157

Wen Fu<sup>‡§</sup>, Diya Shi<sup>‡§</sup>, David Westaway<sup>‡§¶</sup>, and Jack H. Jhamandas<sup>‡§¶</sup>

From the <sup>‡</sup>Division of Neurology, Department of Medicine, <sup>¶</sup>Department of Biochemistry, and <sup>§</sup>Institute of Neuroscience and Mental Health, University of Alberta, Edmonton, Alberta T6G 2S2, Canada

**Background:** Glycolysis in astrocytes may govern amyloid accumulation and cytotoxicity.

**Results:** Inhibiting astrocytic PFKFB3 results in an accumulation of amyloid protein and vulnerability to A $\beta$  cytotoxicity. In APP transgenic mice, reactive astrogliosis parallels the increased A $\beta$  burden and PFKFB3 activity in an age-dependent manner.

**Conclusion:** Astrocytic glycolysis is a key component for amyloid toxicity.

**Significance:** The bioenergetic mechanism in astrocytes may contribute to AD pathology.

Alzheimer disease (AD) is characterized neuropathologically by synaptic disruption, neuronal loss, and deposition of amyloid  $\beta$  (A $\beta$ ) protein in brain structures that are critical for memory and cognition. There is increasing appreciation, however, that astrocytes, which are the major non-neuronal glial cells, may play an important role in AD pathogenesis. Unlike neurons, astrocytes are resistant to A $\beta$  cytotoxicity, which may, in part, be related to their greater reliance on glycolytic metabolism. Here we show that, in cultures of human fetal astrocytes, pharmacological inhibition or molecular down-regulation of a main enzymatic regulator of glycolysis, 6-phosphofructo-2-kinase/fructose-2,6-biphosphatase (PFKFB3), results in increased accumulation of A $\beta$  within and around astrocytes and greater vulnerability of these cells to A $\beta$  toxicity. We further investigated age-dependent changes in PFKFB3 and astrocytes in AD transgenic mice (TgCRND8) that overexpress human A $\beta$ . Using a combination of Western blotting and immunohistochemistry, we identified an increase in glial fibrillary acidic protein expression in astrocytes that paralleled the escalation of the A $\beta$  plaque burden in TgCRND8 mice in an age-dependent manner. Furthermore, PFKFB3 expression also demonstrated an increase in these mice, although at a later age (9 months) than GFAP and A $\beta$ . Immunohistochemical staining showed significant reactive astrogliosis surrounding A $\beta$  plaques with increased PFKFB3 activity in 12-month-old TgCRND8 mice, an age when AD pathology and behavioral deficits are fully manifested. These studies shed light on the unique bioenergetic mechanisms within astrocytes that may contribute to the development of AD pathology.

Alzheimer disease (AD),<sup>2</sup> the most common type of senile dementia, is a progressive neurodegenerative disorder charac-

terized by a gradual deterioration of higher cognitive functions. At a structural level, the brains of AD patients typically exhibit amyloid  $\beta$  (A $\beta$ ) plaques, intracellular neurofibrillary tangles, vascular deposits of amyloid, synaptic disruption, and neuronal loss (1–3). A number of hypotheses have been advanced to explain the pathogenesis of this condition, including disruption of the cell cycle, deposition of misfolded proteins, preferential loss of brain cholinergic neurons, inflammation, oxidative stress, and vascular abnormalities (1). For the last two decades, the AD field has been dominated by the “amyloid hypothesis,” which posits that the accumulation and aggregation of amyloid result in alterations in synaptic function, activation of microglia, release of inflammatory mediators, and oxidative stress (4, 5). These mechanisms culminate in the neuronal dysfunction and degeneration responsible for cognitive deficits in AD. Recently an alternate view has arisen on the basis of a bioenergetics model, proposing that sporadic AD, comprising the majority of cases, is a metabolic disease and that the traditional neuron-centric view of this condition fails to take into account important contributions of non-neuronal cells, particularly astrocytes, to its pathogenesis (6–8).

The presence of reactive astrocytes around A $\beta$  plaques suggests that this phenotype of cells may play an important role in AD pathogenesis (9, 10). Astrocytes can bind and internalize A $\beta$  *in vitro* and *in vivo* and play an important role in plaque formation and maintenance through mechanisms that are not entirely clear (11–13). In contrast to neurons, which are highly vulnerable to A $\beta$  exposure, astrocytes demonstrate relative resistance to A $\beta$  toxicity (14, 15). A comparison of rat neurons and astrocytes reveals a differential bioenergetic response between the two cell types to experimental stimuli (such as nitric oxide or glutamate) that induce cellular stress (16, 17). Upon exposure to these stimuli, neurons undergo a rapid decline in ATP concentration, a collapse in mitochondrial potential ( $\Delta\Psi$ m), and spontaneous apoptotic death. By contrast, astrocytes respond to cellular stressors by increasing their glycolytic metabolism to generate ATP and maintain  $\Delta\Psi$ m. Further stud-

\* This research was supported by grants from Alberta Bio-Solutions (Alberta Prion Research Institute), the Alzheimer's Society of Alberta and Nunavut, and the University Hospital Foundation (FoMD/UHF medical grants competition).

<sup>1</sup> To whom correspondence should be addressed: 530 Heritage Medical Research Centre, Dept. of Medicine (Neurology), University of Alberta, Edmonton, Alberta, T6G 2S2, Canada. Tel.: 780-407-7153; Fax: 780-407-3410; E-mail: jack.jhamandas@ualberta.ca.

<sup>2</sup> The abbreviations used are: AD, Alzheimer disease; A $\beta$ , amyloid  $\beta$ ; PFKFB3, 6-phosphofructo-2-kinase/fructose-2,6-biphosphatase; HFA, fetal human cortical astrocyte; HFN, fetal human cortical neuron; GFAP, glial fibrillary

acidic protein; 3PO, 3-(3-pyridinyl)-1-(4-pyridinyl)-2-propen-1-one; PFK15, 1-(4-pyridinyl)-3-(2-quinolinyl)-2-propen-1-one; MTT, 3-(4,5-dimethylthiazol-2-yl)-2,5-diphenyltetrazolium bromide.

ies ascribe these different responses to the low levels in neurons of isoform 3 of 6-phosphofructo-2-kinase/fructose-2,6-bisphosphatase (PFKFB3), a potent allosteric activator of 6-phosphofructo-1-kinase, which is the rate-limiting enzyme for glycolysis (16). Astrocytes, however, show an abundance of PFKFB3, and use of siRNA targeted against PFKFB3 abolishes the ability of these cells to up-regulate glycolysis in response to stimuli that induce cellular stress (18). On the basis of these observations, we hypothesized that, in astrocytes, impairment of bioenergetic mechanisms involving enzyme PFKFB3 renders these cells vulnerable to A $\beta$  toxicity and promotes A $\beta$  accumulation and plaque formation, a key feature of AD pathogenesis. In this study, we first identified basal levels of the glycolytic enzyme PFKFB3 in primary cell cultures of human fetal astrocytes (HFAs) and neurons. We next examined the role of PFKFB3 in the promotion of A $\beta$  accumulation and plaque formation and the cellular viability of HFAs using pharmacological and siRNA approaches. Finally, we sought to examine the levels of PFKFB3 in TgCRND8 transgenic mice (expressing a mutant human amyloid precursor protein (APP)) *versus* age-matched wild-type mice and to correlate such alterations with age-dependent increases in A $\beta$  plaques observed in TgCRND8 mice.

## EXPERIMENT PROCEDURES

**Cultures of fetal human cortical neurons (HFNs) and HFAs**—Human cortical fetal neurons and astrocytes were isolated as described previously (19, 20). Briefly, neuronal cultures were prepared from gestational week 12–15 fetuses with approval of the Human Ethics Research Board at the University of Alberta. After we removed the meninges and blood vessels, the brain tissue was washed in minimum essential medium and mechanically dissociated by repeated trituration through a 20-gauge needle. Cells were centrifuged at  $1500 \times g$  for 10 min and resuspended in minimum essential medium with 10% heat-inactivated FBS, 0.2% N2 supplement, and 1% penicillin/streptomycin antibiotic solution (Pen-Strep, Gibco). Subsequently, cultures were treated with arabinofuranosylcytosine (25  $\mu$ mol/liter) for 2 weeks. HFN cultures were grown in a 5% CO<sub>2</sub> humidified incubator at 37 °C. To generate enriched primary astrocytes, the cell culture was incubated without arabinofuranosylcytosine. For immunohistochemical experiment, cells were plated for 2–7 days on glass coverslips precoated with poly-L-ornithine (Sigma) or 96-well plates. The age range for the most cells used in this study was 14–42 days *in vitro* (no more than 60 days *in vitro* for HFNs and no more than 90 days *in vitro* for HFAs). Soluble oligomeric A $\beta$ <sub>1–42</sub> and the reverse nonfunctional sequence peptide, A $\beta$ <sub>42–1</sub>, were prepared according to protocols published previously (19), and the oligomerization state of the peptides was, therefore, not measured in this study.

**A $\beta$  Plaque and PFKFB3 Expression in Brain Regions of TgCRND8 APP-overexpressing Mice**—Transgenic animals were obtained from the University of Alberta Centre for Prions and Protein Folding Diseases Animal Facility. Under halothane anesthesia, TgCRND8 APP mice (2, 4, 7, 9, and 12 months of age;  $n = 4$  for each age group) and age-matched control mice ( $n = 4$  for each age group) were decapitated, and the brains were removed quickly. The brains were hemisected, and one half of the brain was used for dissecting the cortex and hip-

pocampus. Tissue was weighed and placed in cold radioimmune precipitation assay buffer (Thermo Scientific Inc., Rockford, IL) with protease inhibitors, and then proteins were isolated and measured using a Bio-Rad protein assay kit. Proteins were diluted with SDS sample buffer (New England Biolabs, Whitby, ON) and loaded at 20–30  $\mu$ g/lane on 10–14% acrylamide gels, depending on the predicted protein size. Proteins were transferred to a nitrocellulose membrane and blocked with LI-COR blocking buffer. Nitrocellulose membranes were incubated with primary antibodies overnight at 4 °C on a shaker and subsequently incubated with IRDye 800CW goat anti-rabbit and IRDye 680CW goat anti-mouse secondary antibodies. The other halves of the brains from TgCRND8 and control mice were fixed for immunohistochemical analysis of brain sections from the cortex and hippocampus to determine A $\beta$  plaque deposition, and the same sections were also double-stained using phospho-PFKFB3 antibody. For determination of A $\beta$  plaque size and distribution, the A $\beta$  (6E10)-immunostained sections were imaged using a Leica SP5 confocal microscope with a  $\times 20/0.5$  lens.

**Fluorescent Immunohistochemistry**—HFAs/HFNs on coverglass were fixed with 4% paraformaldehyde and stained with primary and secondary antibodies. The primary antibodies used were as follows: GFAP and rabbit anti-GFAP polyclonal antibody (Santa Cruz Biotechnology, Inc.); A $\beta$  (6E10) mouse monoclonal antibody (Covance Inc., Montreal, Canada); phospho-PFKFB3 (Ser-467) rabbit monoclonal (Bioss Inc., Woburn, MA); and MAP2 mouse monoclonal antibody (Sigma). The secondary antibodies used were Alexa Fluor 350 goat anti-rabbit, Alexa Fluor 488 chicken anti-rabbit, and Alexa Fluor 546 goat anti-mouse antibody (Invitrogen). Photomicrographs of stained cells were taken using an AxioPlan-2 fluorescence microscope with AxioVision software (Carl Zeiss Ltd., Toronto, ON, Canada) or a FV1000 confocal microscopy with Olympus FluoView software (F10-ASW). Astrocyte morphology and A $\beta$  plaque size were further analyzed with ImageJ software, version 1.49 (<http://imagej.nih.gov/ij/>) (21). Three different batches of HFA/HFN cultures were used, and three to five different fields of view for each batch of cells were analyzed.

**In-cell Western Blot and Western Blot Analyses**—Intracellular signaling profiles were determined using LI-COR in-cell Western blot techniques. HFAs were seeded at 5000 cells/well in a 96-well plate. After culturing for 24 h, cells were pretreated for 24 h with/without 3PO/PFK15 at the indicated concentrations, followed by treatment with A $\beta$ <sub>1–42</sub> in culture medium for another 24 h. Subsequently, cells were fixed with 4% paraformaldehyde for 20 min, permeabilized with 0.2% Triton X-100, blocked with Odyssey blocking buffer (LI-COR), and stained with mouse A $\beta$  (6E10) antibody. The secondary antibody was IRDye 800CW goat anti-mouse antibody, and Sapphire700 and DRAQ5 were used for cell number normalization (LI-COR). Plates were imaged using an Odyssey infrared imaging system (LI-COR), and the integrated intensity was normalized to the total cell number on the same well. For Western blot analysis, protein was loaded at 20–30  $\mu$ g/lane. The primary antibodies used were PFKFB3 (rabbit polyclonal (Abcam, Toronto, ON), mouse monoclonal (Novus Canada, Oakville, ON), phospho-PFKFB3 (rabbit polyclonal, Bioss), GFAP (rabbit polyclonal,

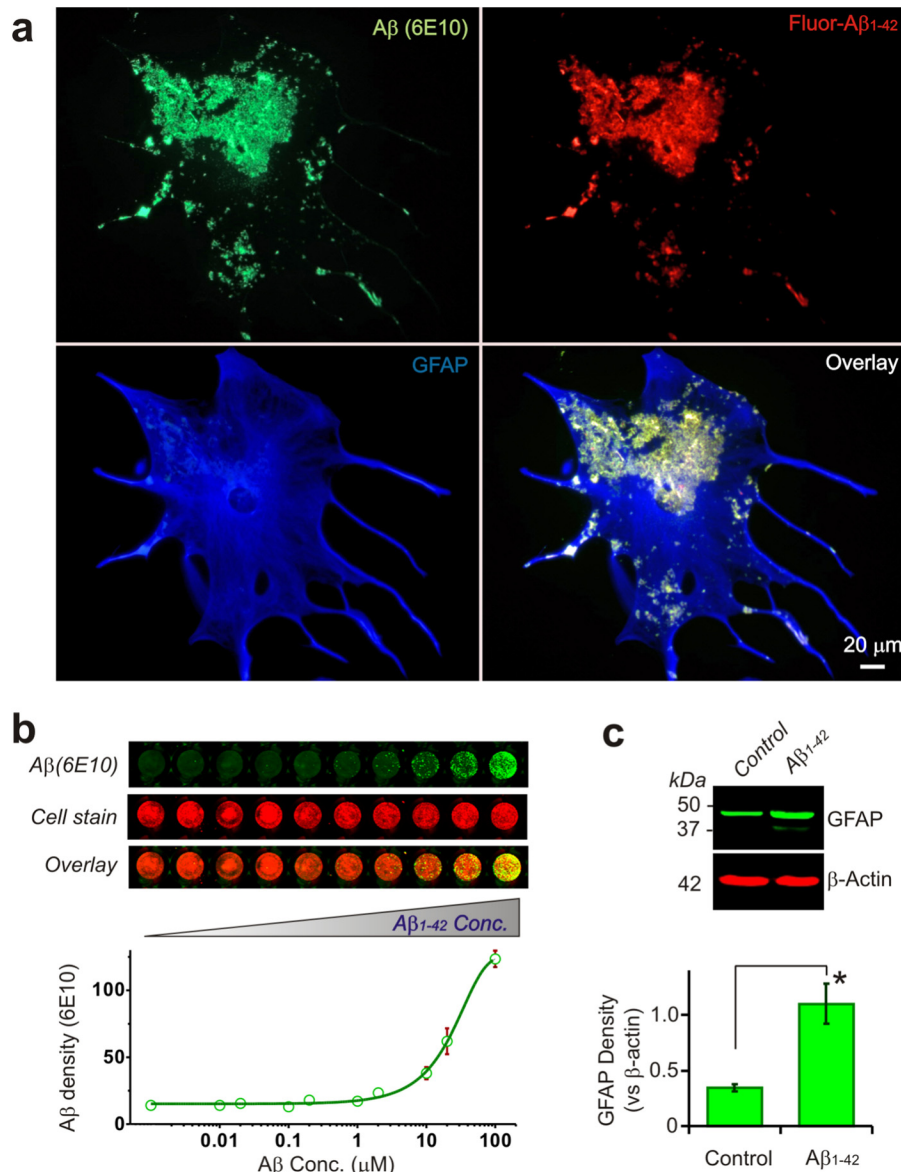


FIGURE 1. **Uptake, accumulation, and amyloid plaque formation in HFAs exposed to A $\beta$ .** *a*, immunofluorescent staining of human fetal astrocytes cultured with fluorescent A $\beta_{1-42}$  (1  $\mu$ M, 24 h) and stained with A $\beta$  (6E10) and GFAP antibody showing that A $\beta_{1-42}$  is taken up into astrocytes and forms plaques that build up on the reactive astrocyte surface. *b*, in-cell-Western blot stained with A $\beta$  (6E10) showing increased A $\beta$  plaque formation followed by increasing extracellular A $\beta_{1-42}$  concentration (Conc.). The Western blot shows that human fetal astrocytes exposed to A $\beta_{1-42}$  become reactive, as characterized by increased GFAP protein expression (*c*, 1  $\mu$ M, 24 h, *n* = 3).

Invitrogen),  $\beta$ -actin (mouse monoclonal, Sigma), and  $\beta$ -tubulin (rabbit polyclonal, Cell Signaling Technology, Inc.). The secondary antibodies used were IRDye 680CW goat anti-mouse antibody and IRDye 800CW goat anti-rabbit antibody (LI-COR). Membranes were scanned and analyzed using the LI-COR Odyssey system.

**Cell Death and Proliferation Assay: MTT Cell Death Assay**—HFAs were seeded to 5000 cells/well in a 96-well plate in minimum essential medium, 10% FBS and incubated overnight. Cells in culture medium were preincubated for 24 h either with or without 3PO/PFK15, followed by treatment with A $\beta_{1-42}$  or A $\beta_{42-1}$  for 24 h. At the end of treatment, 20  $\mu$ l of 5 mg/ml 3-(4,5-dimethylthiazol-2-yl)-2,5-diphenyltetrazolium bromide (MTT, Sigma) was added to each well and incubated at 37  $^{\circ}$ C for 3 h. Medium was removed, 100  $\mu$ l of MTT solvent (isopropanol

with 4 mM HCl) was added to each well, and the plates were incubated for 30 min at room temperature on a rotating shaker. Plates were analyzed on a microplate reader at a 590-nm wavelength. The live/dead assay kit from Invitrogen was used according to the instructions of the manufacturer. HFAs were plated in 24-well plates and treated with 3PO and A $\beta_{1-42}$  as indicated. Cells were analyzed with the GE Healthcare InCell analyzer, and 16 fields/well were imaged and analyzed further with the Investigate software package. The WST-1 proliferation assay kit from Roche was used according to the instructions of the manufacturer.

**siRNA Transfection**—Human PFKFB3 siRNAs used were Trilencer-27 for PFKFB3 (three unique 27-mer siRNA duplexes, OriGene Technologies, Inc., Rockville, MD) and negative control siRNA transfected into HFAs using Lipo-

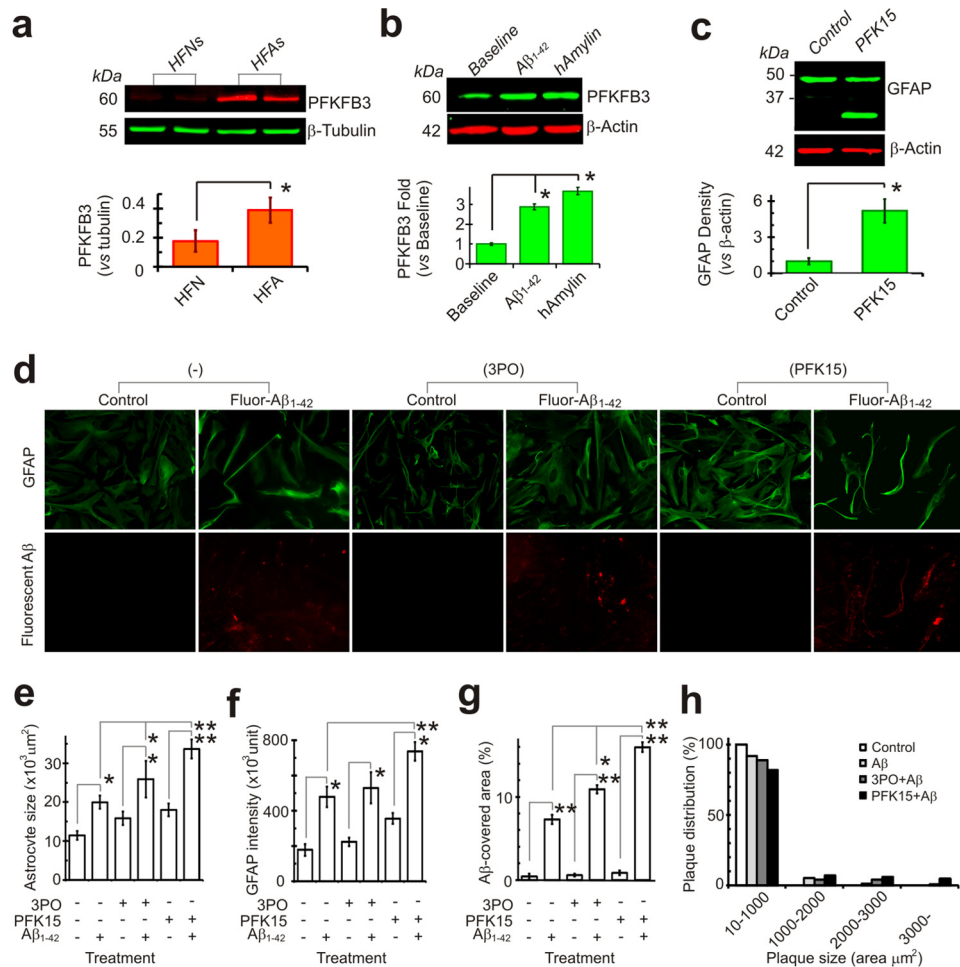


**FIGURE 2. Glycolytic activity affects A $\beta$  uptake and plaque formation in human astrocytes.** *a*, Western blot analysis showing significantly different basal levels of the glycolytic enzyme PFKFB3 in HFNs and HFAs ( $n = 6$ ). *b*, HFAs increase PFKFB3 protein expression after exposure to A $\beta_{1-42}$  (1  $\mu$ M) or human amylin (*hAmylin*, another amyloidogenic peptide, 1  $\mu$ M) for 24 h. *c*, HFAs become “reactive”; that is, characterized by increased GFAP protein expression after metabolic stress, such as inhibition of glycolysis with the PFKFB3 inhibitor PFK15 (20  $\mu$ M, 24 h,  $n = 3$ ). *d*, representative photographs showing that HFA cultures become reactive and demonstrate morphological changes and an increase in GFAP staining after exposure to A $\beta$  or an impairment in glucose metabolism with application of the glycolytic inhibitors 3PO (20  $\mu$ M) or PFK15 (10  $\mu$ M), which further increased A $\beta$  buildup and plaque formation (*e*, *f*, and *g*). The results shown are from five independent experiments. *h*, the glycolytic metabolic stress not only increases A $\beta$  buildup but also results in the formation of larger A $\beta$  plaques. \*,  $p < 0.05$ ; \*\*,  $p < 0.01$ . Scale bars = 20  $\mu$ m.

fectamine RNAiMAX or Lipofectamine 2000 reagent (Invitrogen).

**Other Chemicals and Reagents**—Cell culture reagents were obtained from Invitrogen unless stated otherwise. 3PO was from Merck Millipore (Billerica, MA). PFK15 was from Glaxo Lab (Southborough, MA). DAPI was from Invitrogen. Fluorescent A $\beta_{1-42}$  HiLyte Fluor 555 was from AnaSpec Inc. (Fremont, CA). A $\beta_{1-42}$  and A $\beta_{42-1}$  were from rPeptide (Bogart, GA).

**Statistical Analysis**—Values are means  $\pm$  S.D. Significance was determined using unpaired Student’s *t* test or one-way analysis of variance, followed by Tukey’s test when appropriate, with Prism software (GraphPad Prism 5, GraphPad Software, San Diego, CA).  $p < 0.05$  was considered significant.

## RESULTS

**Astrocytic Involvement in A $\beta$  Clearance and Amyloid Plaque Formation**—Application of fluorescent labeled A $\beta_{1-42}$  to HFAs resulted in a concentration-dependent accumulation of the peptide over the surface of astrocytes to form amyloid plaques (Fig. 1, *a* and *b*). Clearance of the A $\beta$  from the extracellular space

and its internalization within astrocytic processes was also evident (Fig. 1*a*). Sustained exposure of HFAs to A $\beta$  results in conversion to reactive astrocytes that were characterized by cellular hypertrophy and proliferation and increased synthesis of GFAP (Fig. 1, *a* and *c*). The presence of A $\beta_{1-42}$  in culture dishes without HFAs did not result in amyloid plaque formation, nor did we observe any significant internal A $\beta$  within HFAs that were not incubated with exogenous A $\beta_{1-42}$  (data not shown).

**A $\beta$  Plaque Formation Depends on Astrocyte Glycolytic Enzyme PFKFB3 Function**—Astrocytes express much higher levels of PFKFB3 than neurons and demonstrate low levels of APC/C-Cdh1 activity. APC/C-Cdh1 is an E3 ubiquitin ligase that degrades PFKFB3 following ubiquitination. In contrast, neurons express low levels of PFKFB3 but higher levels of APC/C-Cdh1 activity. These distinctions result in astrocytes functioning at a high glycolysis rate and neurons being extremely sensitive to energy depletion and degeneration (22). In our cell culture model, HFAs indeed demonstrated a significantly higher expression of PFKFB3 than HFNs (Fig. 2*a*). In addition to increased levels of GFAP, as shown in Fig. 1*c*, HFAs exposed

## Astrocytic Glycolysis and Amyloid Toxicity

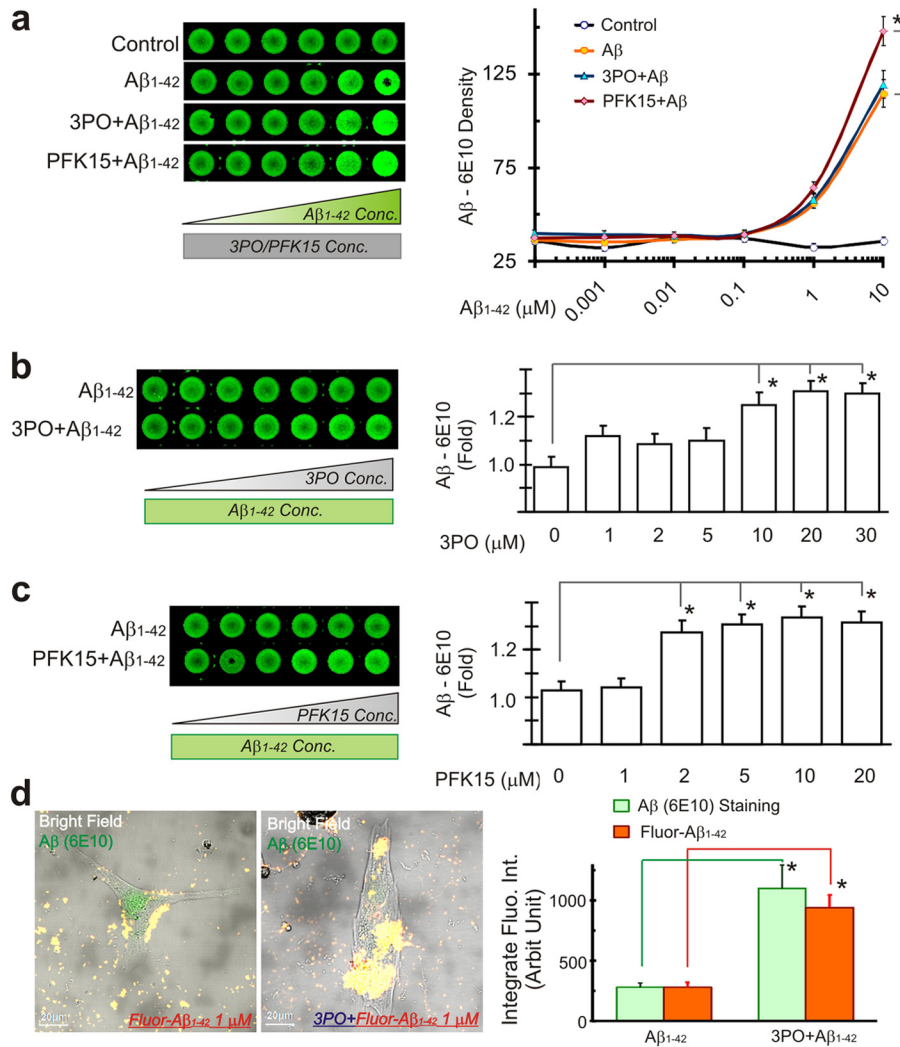


**FIGURE 3. A $\beta$  plaque formation in human fetal astrocytes is correlated with PFKFB3 activity.** *a*, in-cell Western blot stained with A $\beta$  (6E10) showing that deteriorated astrocyte metabolism enhances A $\beta$  plaque formation, followed by glycolysis inhibition with the PFKFB3 inhibitors 3PO (20  $\mu$ M) or PFK15 (10  $\mu$ M). *Conc.*, concentration. *b* and *c*, A $\beta$  plaque formation increases with increasing concentrations of glycolysis inhibitor 3PO (*b*) or PFK15 (*c*) (A $\beta$ <sub>1-42</sub> concentration, 1  $\mu$ M). *d*, using confocal microscopy quantification, A $\beta$  fluorescence increased significantly after glycolysis inhibition with 3PO (20  $\mu$ M, *n* = 9). \*, *p* < 0.05.

to A $\beta$ <sub>1-42</sub> also displayed increased expression of the key glycolytic enzyme PFKFB3, which is indicative of heightened glycolytic activity. Another amyloidogenic peptide, human amylin, also increased astrocytic PFKFB3 expression (Fig. 2*b*). Interestingly, after inhibition of glycolysis with PFK15, a potent PFKFB3 inhibitor (23), HFAs also demonstrated increased expression of GFAP, consistent with reactive astrocytes (Fig. 2, *c* and *d*). Because A $\beta$  plaque formation on astrocytes depends on extracellular A $\beta$  concentration *in vitro* (Fig. 1*b*), we sought to examine whether inhibition of glycolysis influenced A $\beta$  deposition. Following inhibition of glycolysis with either 3PO or PFK15, both PFKFB3 inhibitors, the intensity of GFAP staining in HFAs also increased significantly with formation of larger A $\beta$  plaques (Fig. 2, *e-g*). The A $\beta$  density curves were also shifted to the left (Fig. 3*a*). Furthermore, A $\beta$  plaque formation increased in a concentration-dependent manner following applications of progressively higher concentrations of the glycolytic inhibitors 3PO or PFK15 while maintaining the same concentration of A $\beta$ <sub>1-42</sub> in the extracellular milieu (Fig. 3, *b-d*). Astrocytes in HFA cultures that became reactive also showed morphological

cellular changes and increased GFAP staining after exposure to either A $\beta$  or an impairment of glucose metabolism with application of glycolytic inhibitors (Fig. 3*d*).

**Glycolytic Inhibition Renders Astrocytes Vulnerable to A $\beta$  Toxicity**—In comparison with neurons, astrocytes under normal glucose metabolic conditions are relatively resistant to A $\beta$  cytotoxicity (14). However, an inhibition of glycolytic metabolism in astrocytes renders them vulnerable to cell death upon exposure to A $\beta$ . In HFAs pretreated with PFKFB3 inhibitors (3PO or PFK15), an increase in cell death was observed using three distinct assays of cell viability (Fig. 4, *a-d*). As shown in Fig. 4, *a-d*, the effects of applying either 3PO or PFK15 were dose-dependent. We further confirmed that these changes in astrocyte survival were PFKFB3-specific by using siRNA to specifically down-regulate PFKFB3 protein expression (Fig. 4, *e* and *f*). In HFA cultures where PFKFB3 activity was down-regulated in this manner, an increase in GFAP (indicative of their change to reactive astrocytes) and cell death was observed upon exposure to A $\beta$  at concentrations that normally did not influence cell survival (Fig. 4*e*).

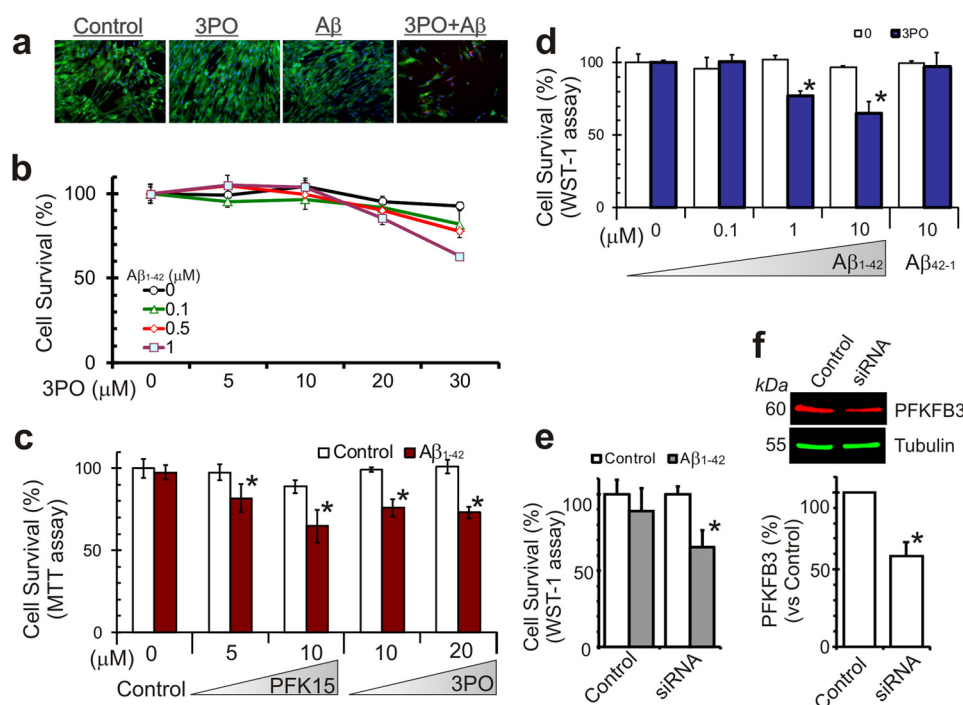


FIGURE 4. **PFKFB3 activity affects  $A\beta$  cytotoxicity in human fetal astrocytes.** *a*, in-cell analysis imaging the live/dead assay with calcein (green, live cells) and ethidium homodimer I (red, dead cells) with human fetal astrocytes cultured with 3PO (20  $\mu$ M) and  $A\beta_{1-42}$  (1  $\mu$ M) for 48 h. *b*, using the live/dead assay and quantifying with InCell analyzer, resting human astrocytes are not sensitive to  $A\beta$  cytotoxicity. However, astrocytes had increased sensitivity to  $A\beta$  cytotoxicity after PFKFB3 activity was inhibited with 3PO. *c*, using an MTT proliferation assay, increased  $A\beta$  induced astrocyte cell death after metabolic stress when PFKFB3 activity was inhibited with PFK15 or 3PO. *d*, another proliferation assay (WST-1) showed similar increased  $A\beta$  toxicity following glycolysis inhibition with 3PO (20  $\mu$ M, 24 h) but not the reverse sequence peptide  $A\beta_{42-1}$ . *e* and *f*, the increased  $A\beta$  cytotoxicity after PFKFB3 inhibition is PFKFB3-specific because it is down-regulated with PFKFB3 siRNA transfection in these cells. \*,  $p < 0.05$ .

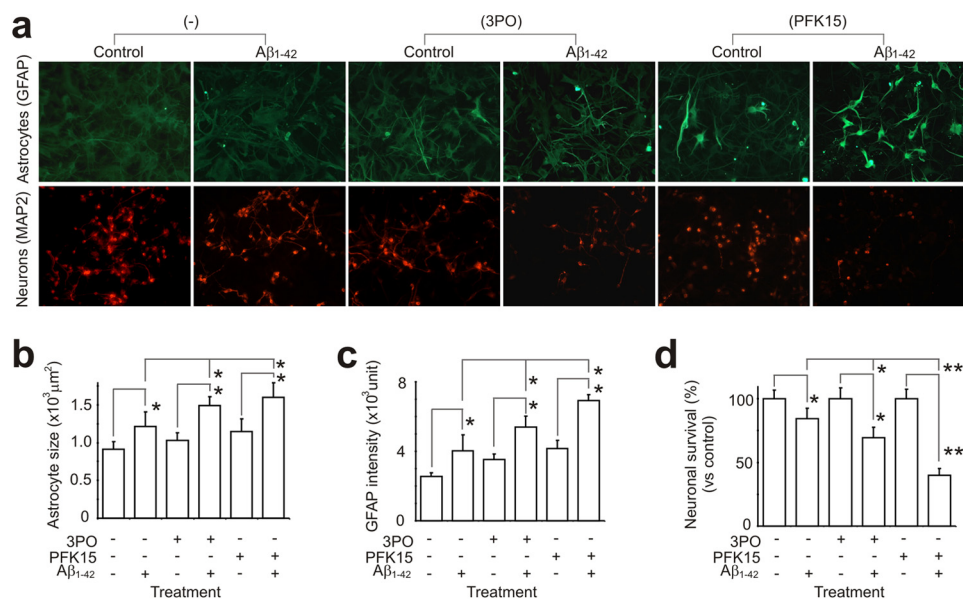


FIGURE 5. **PFKFB3 activity is important for  $A\beta$  cytotoxicity in a mixed culture of human fetal neurons and astrocytes.** *a*, in cocultured HFNs and HFAs, HFAs maintain a homeostatic environment and keep HFNs healthy. *b* and *c*, after *b* and *c* and have decreased capability to maintain the microenvironment, resulting in a gradual loss of HFNs. *d*, when these stressed HFAs are exposed to  $A\beta$ , they become more sensitive to  $A\beta$  cytotoxicity, resulting in a further loss of their capability to support neurons and, hence, increased neuronal cell death (3PO, 20  $\mu$ M; PFK15, 10  $\mu$ M;  $A\beta_{1-42}$ , 1  $\mu$ M; 24 h). \*,  $p < 0.05$ ; \*\*,  $p < 0.01$ . Scale bar = 20  $\mu$ m.

In co-cultures of HFAs and HFNs, where astrocytes provide a homeostatic environment to keep neurons healthy (20), an inhibition of PFKFB3 function (application of 3PO or PFK15), HFAs demonstrated reactive astrogliosis (Fig. 5, *a–c*). These reactive HFAs developed increased vulnerability when exposed to  $A\beta$  (they became more reactive with stronger GFAP staining,

Fig. 5, *a–c*) and a decreased capability to maintain glial-neuronal homeostasis that resulted in neuronal death (Fig. 5, *a* and *d*).

**PFKFB3 Activity Is Involved in  $A\beta$  Plaque Formation in the Transgenic AD Mouse Model**—TgCRND8 mice carry combined APP Swedish (K670M/N671L) and Indiana (V717F) mutations, resulting in an aggressive neuropathology evident

## Astrocytic Glycolysis and Amyloid Toxicity

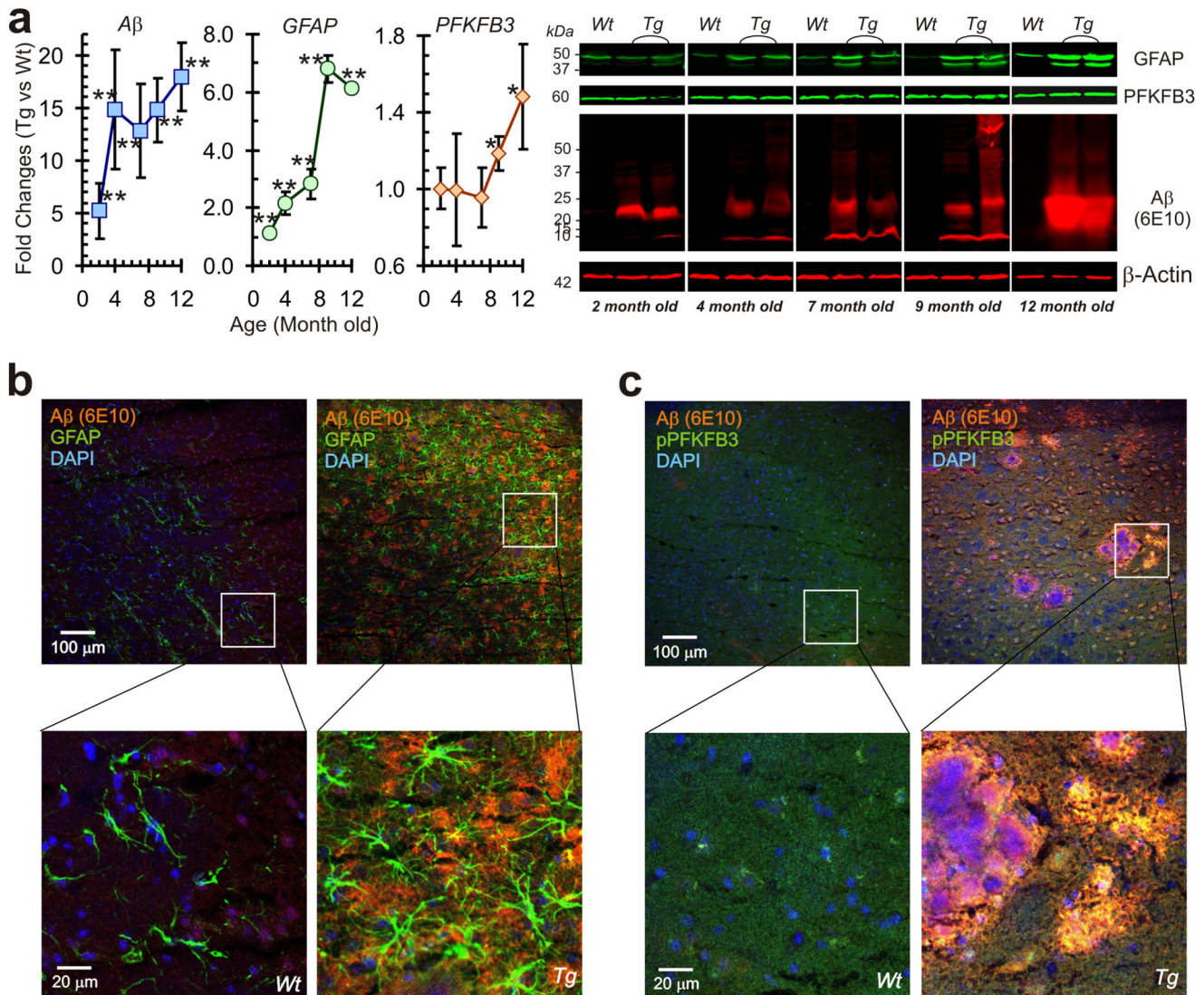


**FIGURE 6. Temporal changes in A $\beta$ , GFAP, and PFKFB3 expression in AD transgenic mice (TgCRND8).** *a*, Western blot analyses for GFAP, PFKFB3, and A $\beta$  protein expression from the cortex of transgenic AD mouse brain (TgCRND8) compared with the age-matched wild type ( $n = 4$  for each group). Quantitative changes in GFAP, PFKFB3, and A $\beta$  protein expression in wild-type and TgCRND8 mice over time (in months) are depicted in the *left panels*. *b*, immunofluorescence staining of 12-month-old AD mouse brain with A $\beta$  (6E10) and GFAP antibodies showing A $\beta$  plaque surrounded closely by enlarged and stronger GFAP-stained astrocytes (*right panels*), whereas the age-matched wild-type mouse brain shows no significant plaque formation and reactive astrogliosis (*left panels*). *c*, in AD mouse brain (*right panels*), increased phospho-PFKFB3 (*green*) surrounds and is colocalized with A $\beta$  plaques (*red*), shown as *yellow*, whereas the age-matched wild-type mouse brain shows weak PFKFB3 activity ( $n = 4$  for each group). \*,  $p < 0.05$ ; \*\*,  $p < 0.01$ .

by 3 months of age, and, by 6 months of age, animals demonstrate large numbers of diffuse and plaque amyloid deposits (24). Therefore, in TgCRND8 mice, we examined age-dependent increases in reactive astrocytes (as measured by GFAP expression) and the glycolytic profile (as measured by PFKFB3 expression). In the same animals, we also assessed the amyloid burden with immunohistochemistry and Western blot analysis. In TgCRND8 mice, an increase in A $\beta$  load was seen as early as 2 month of age (Fig. 6*a*), followed by increased GFAP protein expression from about 4 months of age, indicative of reactive astrogliosis. An increase in PFKFB3 protein expression followed at a later age, after 9 months. Immunohistochemical staining showed significant reactive astrogliosis surrounding A $\beta$  plaque with increased PFKFB3 activity in these aged (12-month-old) AD mice (Fig. 6, *b* and *c*).

To mimic the above *in vivo* sequence of events in our HFA culture model system, we first incubated HFAs with soluble

oligomeric A $\beta_{1-42}$  for 12 h, which resulted in early amyloid plaque formation. Subsequent applications of the glycolytic inhibitor PFK15 resulted in a concentration-dependent acceleration and increase in amyloid plaque formation (Fig. 7).

## DISCUSSION

Bioenergetic mechanisms and neuronal-astrocytic interplay are increasingly viewed as important elements in the pathogenesis of aging and AD (7, 10). Brain glucose uptake and metabolism both decline with the aging process and are accompanied by a decrease in glycolysis (25, 26). This hypometabolism of glucose as an energy substrate is also viewed as an early event in the genesis of AD (27) and may, in fact, represent a general phenomenon for many neurodegenerative diseases (28, 29). For decades, AD has been considered to arise mainly because of specific dysfunction and pathology affecting neurons. This neuron-centric view has been challenged recently by a "neuroener-

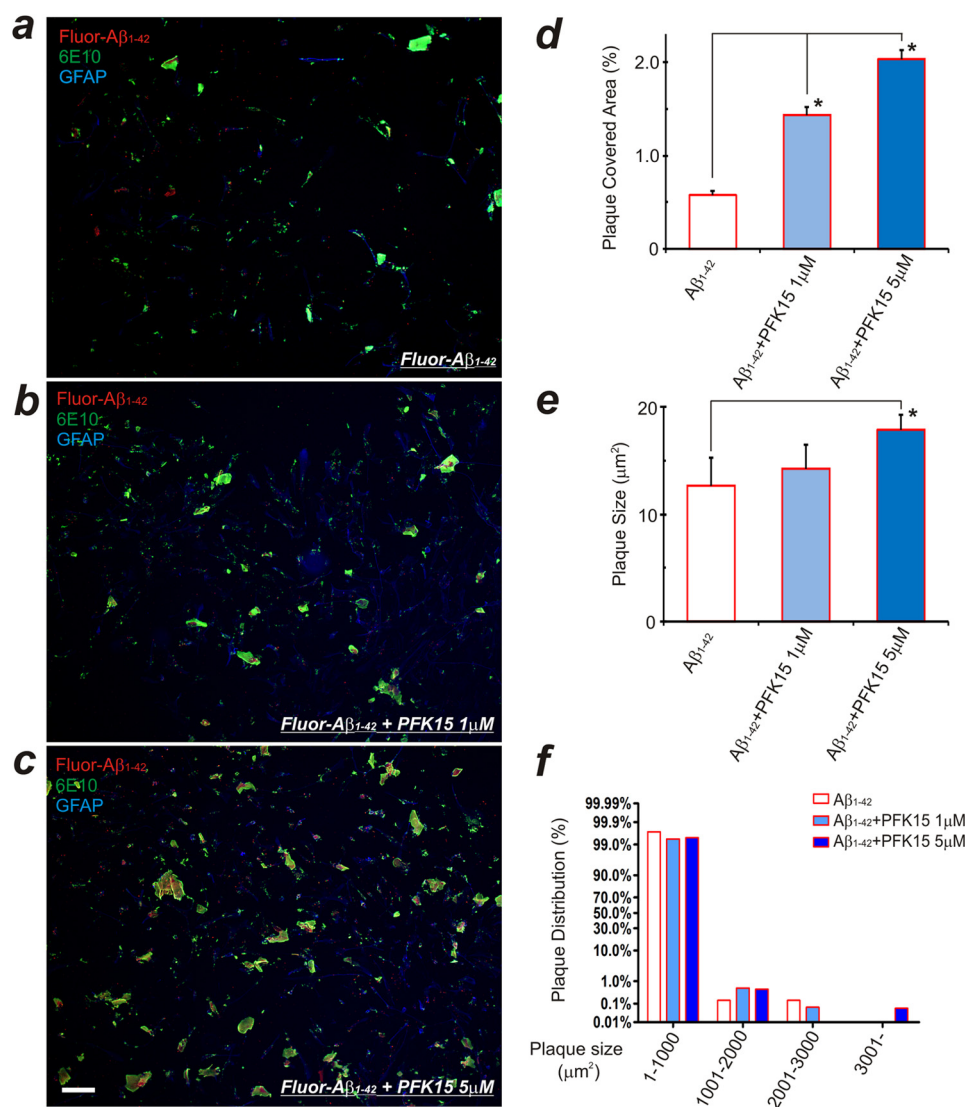


FIGURE 7. **Delayed glycolysis inhibition further enhances plaque formation in HFAs.** *a*, HFAs cultured with 200 nM Fluor-Aβ<sub>1-42</sub> for 12 h forms Aβ plaques. *b* and *c*, with continued application of Fluor-Aβ<sub>1-42</sub>, delayed inhibition of glycolysis with the PFKFB3 inhibitor PFK15 (1 or 5 μM) for another 24 h results in accelerated and increased amyloid plaque formation. The increase in the plaque-covered area (*d*) and plaque size and distribution (*e* and *f*) appear to be correlated with the concentration of PFK15 that is applied. Results from three separate experiments with different batches of cultured HFAs were analyzed. \*,  $p < 0.05$  compared with the Aβ control group. Scale bar = 100 μm.

getic hypothesis" (30), which serves to incorporate changes in the metabolic machinery of astrocytes as an important step in the neurodegenerative processes that unfold during AD (31–33). In this study, we demonstrate, for the first time, that, in HFAs, impairment of glycolysis promotes an increase in amyloid aggregation and internalization within these glial cells. Furthermore, inhibition of glycolysis renders the normally resistant human astrocytes vulnerable to Aβ toxicity. Finally, in a transgenic mouse model of AD, we identify that increased reactive astrogliosis (as measured by GFAP expression) and amyloid deposition precede the increase in the key glycolytic enzyme PFKFB3.

Astrocytes undergo functional decline with age (senescence) that can be recapitulated, in part, when such cells are exposed *in vitro* to stressful stimuli such as oxidative stress or exposure to Aβ peptides (34). When exposed to Aβ, in addition to internalization and accumulation of this peptide, HFAs demonstrate a change in metabolic phenotype characterized by up-regulation

of PFKFB3, which is the rate-limiting enzyme for glycolysis via the 6-phosphofructo-1-kinase pathway. This initial increase in glycolysis within HFAs may be viewed as a compensatory homeostatic mechanism to produce increased energy substrate in the form of lactate, which provides an additional source of energy for neurons under conditions when oxidative phosphorylation activity is impaired, *i.e.* in the presence of Aβ or other stressors. Impairment of the glycolytic enzyme PFKFB3, either pharmacologically (with 3PO or PFK15) or by silencing PFKFB3 at the mRNA level with siRNA transfection of HFAs, resulted in significant cell death of astrocytes when exposed to Aβ, as measured using three independent cell survival assays.

Reactive astrogliosis is a well characterized spectrum of morphological and biochemical changes that occur in astrocytes in response to a variety of insults (35) and has also been identified in the context of stress-induced astrocyte senescence (36). In the brains of AD patients, an increase in glycolytic enzymes is correlated with elevated GFAP expression in astrocytes, sug-



## Astrocytic Glycolysis and Amyloid Toxicity

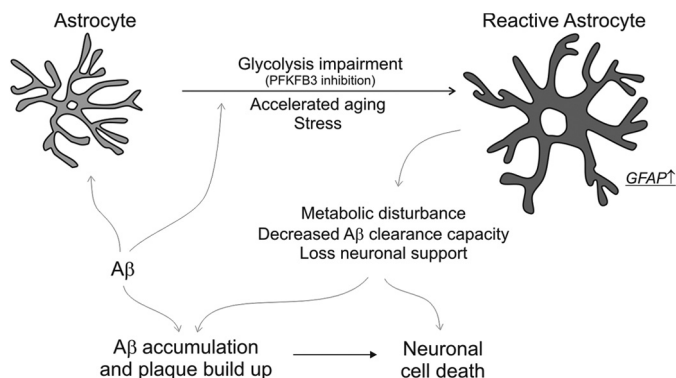


**FIGURE 8. Astrocytic bioenergetic mechanisms contribute to amyloid accumulation and neuronal death.** The schematic depicts the transformation of astrocytes to a reactive state when exposed to A $\beta$  protein, a process that is augmented by loss of glycolytic function (PFKFB3 inhibition), accelerated aging, or cellular stress. The homeostatic disturbance that ensues in reactive astrocytes (identified by an increase in GFAP) results in a loss of neuronal metabolic support and an inability to clear A $\beta$  protein. These changes lead to accumulation of A $\beta$  and adversely impact neuronal function, resulting in neurodegeneration.

gesting that up-regulation of glycolysis may, in part, be a result of reactive astrocytosis that develops with advancing AD (37). In a recent study, several GFAP isoforms have been shown to be up-regulated in a concerted manner in the human AD brain (38). Our results also show an overall increase in total GFAP levels after exposure to A $\beta_{1-42}$  (Fig. 1c) following compromise of glycolysis in cultured HFAs (Fig. 2c) and, additionally, in an age-dependent manner in the AD mouse brain (Fig. 6a). We suspect that the multiple bands we observed on the Western blots correspond to different GFAP isoforms described in a recent report (38), although we did not characterize this further. Interestingly, such changes in glycolysis also correlate spatially with A $\beta$  deposition in PET imaging studies on the human brain (39). Our *in vivo* data from transgenic AD mice (TgCRND8) that overexpress amyloid and develop cognitive impairment in an age-dependent manner suggest that PFKFB3, a key regulatory enzyme for the initiation of glycolysis, may play an important role in AD pathogenesis. We observed an increase in amyloid burden in TgCRND8 mice that preceded similar increases in GFAP expression in AD mice over age-matched wild-type controls. At  $\sim$ 7 months, we noticed an increase in PFKFB3 levels in the brains of TgCRND8 mice compared with control mice. Immunohistochemical staining confirmed a close anatomical relationship between reactive astrocytes and PFKFB3 expression within the same cells that surround and are intermingled with amyloid plaques (Fig. 6, b and c). The sequence of temporal changes in amyloid levels and GFAP and PFKFB3 activity observed in transgenic AD mice fit with our *in vitro* data in HFA cultures and suggest that sustained amyloid exposure of astrocytes leads to increased reactive astrogliosis followed by a slower induction of glycolysis, as measured by PFKFB3 levels. Our histological analysis in TgCRND8 AD mice does not allow us to exclude contributions of neuronal PFKFB3 in disease progression. However, basal levels of PFKFB3 in the neurons under normal conditions are quite low compared with astrocytes and neuronal glycolysis, therefore accounting for only a small portion of the energy demand (16, 17). On the basis of our *in vitro* and *in vivo* data, the impact of A $\beta$  on astrocytic

bioenergetic mechanisms and the consequences of this interplay on neuronal survival are summarized in Fig. 8.

Neoplastic transformation in cells causes a marked increase in glycolytic activity even under normoxic conditions, a phenomenon originally termed the Warburg effect (40). Recently, small molecule inhibitors of PFKFB3, such as 3PO and PFK15, have been developed to promote cytostasis and inhibit tumorigenic growth *in vivo* (23, 41). On the basis of our studies, an undesired consequence of this strategy for cancer treatment may consist of impairment of astroglial glycolytic metabolism and, as a result, a downstream decrease in neuronal viability that depends intimately on healthy, synergistic neuron-astrocyte interactions.

*Acknowledgments*—We thank Jing Yang for assistance with transgenic TgCRND8 mice and Dave MacTavish and Beipei Shi for technical assistance.

## REFERENCES

1. Querfurth, H. W., and LaFerla, F. M. (2010) Alzheimer's disease. *N. Engl. J. Med.* **362**, 329–344
2. Serrano-Pozo, A., Frosch, M. P., Masliah, E., and Hyman, B. T. (2011) Neuropathological alterations in Alzheimer disease. *Cold Spring Harb. Perspect. Med.* **1**, a006189
3. Skovronsky, D. M., Lee, V. M., and Trojanowski, J. Q. (2006) Neurodegenerative diseases: new concepts of pathogenesis and their therapeutic implications. *Annu. Rev. Pathol.* **1**, 151–170
4. Selkoe, D. J. (2008) Biochemistry and molecular biology of amyloid  $\beta$ -protein and the mechanism of Alzheimer's disease. *Handb. Clin. Neurol.* **89**, 245–260
5. Hardy, J. (2009) The amyloid hypothesis for Alzheimer's disease: a critical reappraisal. *J. Neurochem.* **110**, 1129–1134
6. Swerdlow, R. H. (2007) Is aging part of Alzheimer's disease, or is Alzheimer's disease part of aging? *Neurobiol. Aging* **28**, 1465–1480
7. Demetrius, L. A., and Driver, J. (2013) Alzheimer's as a metabolic disease. *Biogerontology* **14**, 641–649
8. Demetrius, L. A., and Simon, D. K. (2012) An inverse Warburg effect and the origin of Alzheimer's disease. *Biogerontology* **13**, 583–594
9. Maragakis, N. J., and Rothstein, J. D. (2006) Mechanisms of disease: astrocytes in neurodegenerative disease. *Nat. Clin. Pract. Neurol.* **2**, 679–689
10. Sofroniew, M. V., and Vinters, H. V. (2010) Astrocytes: biology and pathology. *Acta Neuropathol.* **119**, 7–35
11. Nagele, R. G., D'Andrea, M. R., Lee, H., Venkataraman, V., and Wang, H. Y. (2003) Astrocytes accumulate A  $\beta$  42 and give rise to astrocytic amyloid plaques in Alzheimer disease brains. *Brain Res.* **971**, 197–209
12. Nielsen, H. M., Veerhuis, R., Holmqvist, B., and Janciauskiene, S. (2009) Binding and uptake of A  $\beta$  1–42 by primary human astrocytes *in vitro*. *Glia* **57**, 978–988
13. Friedrich, R. P., Tepper, K., Röncke, R., Soom, M., Westermann, M., Reymann, K., Kaether, C., and Fändrich, M. (2010) Mechanism of amyloid plaque formation suggests an intracellular basis of A $\beta$  pathogenicity. *Proc. Natl. Acad. Sci. U.S.A.* **107**, 1942–1947
14. Pike, C. J., Burdick, D., Walencewicz, A. J., Glabe, C. G., and Cotman, C. W. (1993) Neurodegeneration induced by  $\beta$ -amyloid peptides *in vitro*: the role of peptide assembly state. *J. Neurosci.* **13**, 1676–1687
15. Garwood, C. J., Pooler, A. M., Atherton, J., Hanger, D. P., and Noble, W. (2011) Astrocytes are important mediators of A $\beta$ -induced neurotoxicity and tau phosphorylation in primary culture. *Cell Death Dis.* **2**, e167
16. Bolaños, J. P., Almeida, A., and Moncada, S. (2010) Glycolysis: a bioenergetic or a survival pathway? *Trends Biochem. Sci.* **35**, 145–149
17. Allaman, I., Bélanger, M., and Magistretti, P. J. (2011) Astrocyte-neuron metabolic relationships: for better and for worse. *Trends Neurosci.* **34**, 76–87
18. Herrero-Mendez, A., Almeida, A., Fernández, E., Maestre, C., Moncada,

- S., and Bolaños, J. P. (2009) The bioenergetic and antioxidant status of neurons is controlled by continuous degradation of a key glycolytic enzyme by APC/C-Cdh1. *Nat. Cell Biol.* **11**, 747–752
19. Jhamandas, J. H., Li, Z., Westaway, D., Yang, J., Jassar, S., and MacTavish, D. (2011) Actions of  $\beta$ -amyloid protein on human neurons are expressed through the amylin receptor. *Am. J. Pathol.* **178**, 140–149
  20. Fu, W., Ruangkittisakul, A., MacTavish, D., Baker, G. B., Ballanyi, K., and Jhamandas, J. H. (2013) Activity and metabolism-related  $\text{Ca}^{2+}$  and mitochondrial dynamics in co-cultured human fetal cortical neurons and astrocytes. *Neuroscience* **250**, 520–535
  21. Grathwohl, S. A., Kälin, R. E., Bolmont, T., Prokop, S., Winkelmann, G., Kaeser, S. A., Odenthal, J., Radde, R., Eldh, T., Gandy, S., Aguzzi, A., Staufenbiel, M., Mathews, P. M., Wolburg, H., Heppner, F. L., and Jucker, M. (2009) Formation and maintenance of Alzheimer's disease  $\beta$ -amyloid plaques in the absence of microglia. *Nat. Neurosci.* **12**, 1361–1363
  22. Almeida, A., Moncada, S., and Bolaños, J. P. (2004) Nitric oxide switches on glycolysis through the AMP protein kinase and 6-phosphofructo-2-kinase pathway. *Nat. Cell Biol.* **6**, 45–51
  23. Clem, B. F., O'Neal, J., Tapolsky, G., Clem, A. L., Imbert-Fernandez, Y., Kerr, D. A., 2nd, Klarer, A. C., Redman, R., Miller, D. M., Trent, J. O., Telang, S., and Chesney, J. (2013) Targeting 6-phosphofructo-2-kinase (PFKFB3) as a therapeutic strategy against cancer. *Mol. Cancer Ther.* **12**, 1461–1470
  24. Chishti, M. A., Yang, D. S., Janus, C., Phinney, A. L., Horne, P., Pearson, J., Strome, R., Zuker, N., Loukides, J., French, J., Turner, S., Lozza, G., Grilli, M., Kunicki, S., Morissette, C., Paquette, J., Gervais, F., Bergeron, C., Fraser, P. E., Carlson, G. A., George-Hyslop, P. S., and Westaway, D. (2001) Early-onset amyloid deposition and cognitive deficits in transgenic mice expressing a double mutant form of amyloid precursor protein 695. *J. Biol. Chem.* **276**, 21562–21570
  25. Ding, F., Yao, J., Rettberg, J. R., Chen, S., and Brinton, R. D. (2013) Early decline in glucose transport and metabolism precedes shift to ketogenic system in female aging and Alzheimer's mouse brain: implication for bioenergetic intervention. *PLoS ONE* **8**, e79977
  26. Yao, J., Rettberg, J. R., Klosinski, L. P., Cadenas, E., and Brinton, R. D. (2011) Shift in brain metabolism in late onset Alzheimer's disease: implications for biomarkers and therapeutic interventions. *Mol. Aspects Med.* **32**, 247–257
  27. Tomi, M., Zhao, Y., Thamotharan, S., Shin, B. C., and Devaskar, S. U. (2013) Early life nutrient restriction impairs blood-brain metabolic profile and neurobehavior predisposing to Alzheimer's disease with aging. *Brain Res.* **1495**, 61–75
  28. Ferreira, I. L., Resende, R., Ferreira, E., Rego, A. C., and Pereira, C. F. (2010) Multiple defects in energy metabolism in Alzheimer's disease. *Curr. Drug Targets* **11**, 1193–1206
  29. Liang, W. S., Reiman, E. M., Valla, J., Dunckley, T., Beach, T. G., Grover, A., Niedzielko, T. L., Schneider, L. E., Mastroeni, D., Caselli, R., Kukull, W., Morris, J. C., Hulette, C. M., Schmechel, D., Rogers, J., and Stephan, D. A. (2008) Alzheimer's disease is associated with reduced expression of energy metabolism genes in posterior cingulate neurons. *Proc. Natl. Acad. Sci. U.S.A.* **105**, 4441–4446
  30. Demetrius, L. A., and Simon, D. K. (2013) The inverse association of cancer and Alzheimer's: a bioenergetic mechanism. *J. R. Soc. Interface* **10**, 20130006
  31. Heneka, M. T., Rodríguez, J. J., and Verkhratsky, A. (2010) Neuroglia in neurodegeneration. *Brain Res. Rev.* **63**, 189–211
  32. Rossi, D., and Volterra, A. (2009) Astrocytic dysfunction: insights on the role in neurodegeneration. *Brain Res. Bull.* **80**, 224–232
  33. Verkhratsky, A., Sofroniew, M. V., Messing, A., deLanerolle, N. C., Rempé, D., Rodríguez, J. J., and Nedergaard, M. (2012) Neurological diseases as primary gliopathies: a reassessment of neurocentrism. *ASN Neuro.* **4**, e00082
  34. Lynch, A. M., Murphy, K. J., Deighan, B. F., O'Reilly, J. A., Gun'ko, Y. K., Cowley, T. R., Gonzalez-Reyes, R. E., and Lynch, M. A. (2010) The impact of glial activation in the aging brain. *Aging Dis.* **1**, 262–278
  35. Hamby, M. E., and Sofroniew, M. V. (2010) Reactive astrocytes as therapeutic targets for CNS disorders. *Neurotherapeutics* **7**, 494–506
  36. Bhat, R., Crowe, E. P., Bitto, A., Moh, M., Katsetos, C. D., Garcia, F. U., Johnson, F. B., Trojanowski, J. Q., Sell, C., and Torres, C. (2012) Astrocyte senescence as a component of Alzheimer's disease. *PLoS ONE* **7**, e45069
  37. Bigl, M., Brückner, M. K., Arendt, T., Bigl, V., and Eschrich, K. (1999) Activities of key glycolytic enzymes in the brains of patients with Alzheimer's disease. *J. Neural. Transm.* **106**, 499–511
  38. Kamphuis, W., Middeldorp, J., Kooijman, L., Sluijs, J. A., Kooi, E. J., Moeton, M., Freriks, M., Mizee, M. R., and Hol, E. M. (2014) Glial fibrillary acidic protein isoform expression in plaque related astrogliosis in Alzheimer's disease. *Neurobiol. Aging* **35**, 492–510
  39. Vlassenko, A. G., Vaishnavi, S. N., Couture, L., Sacco, D., Shannon, B. J., Mach, R. H., Morris, J. C., Raichle, M. E., and Mintun, M. A. (2010) Spatial correlation between brain aerobic glycolysis and amyloid- $\beta$  (A $\beta$ ) deposition. *Proc. Natl. Acad. Sci. U.S.A.* **107**, 17763–17767
  40. Koppenol, W. H., Bounds, P. L., and Dang, C. V. (2011) Otto Warburg's contributions to current concepts of cancer metabolism. *Nat. Rev. Cancer* **11**, 325–337
  41. Clem, B., Telang, S., Clem, A., Yalcin, A., Meier, J., Simmons, A., Rasku, M. A., Arumugam, S., Dean, W. L., Eaton, J., Lane, A., Trent, J. O., and Chesney, J. (2008) Small-molecule inhibition of 6-phosphofructo-2-kinase activity suppresses glycolytic flux and tumor growth. *Mol. Cancer Ther.* **7**, 110–120